

General Disclaimer

One or more of the Following Statements may affect this Document

- This document has been reproduced from the best copy furnished by the organizational source. It is being released in the interest of making available as much information as possible.
- This document may contain data, which exceeds the sheet parameters. It was furnished in this condition by the organizational source and is the best copy available.
- This document may contain tone-on-tone or color graphs, charts and/or pictures, which have been reproduced in black and white.
- This document is paginated as submitted by the original source.
- Portions of this document are not fully legible due to the historical nature of some of the material. However, it is the best reproduction available from the original submission.

A SIZE-FREQUENCY STUDY OF LARGE
MARTIAN CRATERS

Alexander Woronow*

Department of Geological Sciences,
Harvard University, Cambridge, MA.

(NASA-CR-145858) A SIZE-FREQUENCY STUDY OF
LARGE MARTIAN CRATERS (Harvard Univ.) 47 P
HC \$4.00 CSCI 03E

N76-14003

Unclas
G3/91 03925

* Current address: Lunar and Planetary Laboratory,
University of Arizona
Tucson, Arizona 85721



ABSTRACT

Martian craters in the size range 10 to 250 km follow a log-normal size-frequency distribution law more closely than the heretofore accepted linear relationship between the log of the crater diameter and the log of the crater density. Analysis techniques based on the log-normal model yield possible evidence for the size-frequency evolution of crater-producing bodies.

Some regions on Mars display excessive depletion of either large or small craters; the most likely causes of the depletion are considered. Apparently, eolian sedimentation has markedly altered the population of the small craters south of -30° latitude. The general effects of crater obliteration in the southern hemisphere appear to be confined to diameters of less than 20 km. A strong depletion of large craters in a large region just south of Deuteronilus Mensae, and in a small region centered at 35° latitude and 10° west longitude, may indicate locations of subsurface ice.

BACKGROUND OF CRATER SIZE-FREQUENCY STUDIES

Thomas L. MacDonald (1931) was apparently the first to suggest that for lunar craters the log of the crater density is a linear function of the log of the crater diameter. Since that time virtually all crater size-frequency population analyses of lunar and martian craters have assumed the explicit validity of this log-log (LL) relationship. Most researchers have attributed any deviations from this presumed initial distribution of diameters to physical processes acting subsequent to crater formation. Piotrowski (1953) and J. Jones (1968) developed a posteriori theories to explain the inevitability of the LL relationship for asteroid diameters, although the physical processes that they invoked were admittedly not realistic. The underlying assumption was that in an asteroid-asteroid collision all of the kinetic energy is utilized in the complete pulverization of the entire smaller body plus some fraction of the larger body. The products of pulverization undergo no subsequent collisions, and only one body, the undisturbed fragment of the larger asteroid, remains to interact with yet another asteroid. Considerable mathematical simplifications yield an asymptotically LL distribution of asteroid masses which is then superimposed on a planet, leading to a LL crater size-frequency distribution. The authors invoked this model because they could find no method to describe the size-frequency distribution of the fragments resulting from such collisions.

Kolmogoroff (1941) considered the problem of the observed log-normal (LN) size-frequency distribution of comminution products. He made two assumptions about the breakage process and an asymptotically log-normal size-frequency distribution function resulted from his analysis. The

assumptions are (a) in any interval of time all bodies have an equal probability of being broken, and (b) the fractional sizes of the products are random and independent of the past history of the bodies. These postulates may not be the only ones that lead to a LN size-frequency distribution, but the assumptions are physically plausible for asteroid-asteroid collisions. Observations of the statistical distribution of large craters on Mars verify the LN nature of the size-frequency distribution and are therefore consistent with Kolmogoroff's model (Woronow, 1975).

THE DATA SET

Unless specifically stated otherwise, all analyses will employ a data set consisting of nearly 10,000 martian craters in a latitude band from +65° (North) to -65° (South), and with diameters in the range 10 to 250 km. These craters were hand-measured on USGS quadrangle maps refined to either the controlled or semi-controlled level. All data were stored by 5° latitude x 5° longitude blocks on a PDP-11/DEC tape file, and processed with a PDP-11 computer. For comparative purposes, Figure 1 shows the data plotted on log-log axes in a manner analogous to that suggested by K. L. Jones (1974); and it agrees well with the data set which he presents. This plot would commonly be interpreted as consisting of two straight line segments of the form

$$\text{LOG (crater density)} = m \cdot \text{LOG (crater diameter)} + b$$

which intersect at approximately 20 km diameter: the large craters lying along a -3 slope ($m = -3$), which is presumed to represent the form of the initial distribution, and the small craters lying approximately along a -2 slope, considered an effect of erosion (e.g. Hartmann, 1973). Saturation in the 10-250 km diameter range is not a problem (Hartmann, 1973, Figure 3).

NATURE OF THE LOG-NORMAL DISTRIBUTION FUNCTION

Undoubtedly, the wide acceptance of the LL based analyses is due in part to the graphical ease and mathematical simplicity it offers. An understanding of the LN distribution function's properties, origins, and uses is essential if the analytical techniques are to be grasped intuitively. Only the most salient points are summarized in this section; a thorough treatment can be found in Aitchison and Brown (1973); also Epstein (1947) presents a helpful review of Kolmogoroff's paper on breakage products.

Curve A in Figure 2 is a LN frequency curve. For any value of the abscissa the curve represents the frequency of occurrence of that value. The distribution has been normalized so that the area under the curve equals unity (i.e., any sampled value of the variate has a probability of one that its value will lie between zero and plus infinity).

For crater statistics, the LN distribution has two important differences from the LL distribution: (a) because the area under the LN curve can be normalized, the total number of craters is necessarily finite. (The LL relationship, in its broadest interpretation, predicts an infinity of craters). (b) At zero diameter the number of craters goes to zero in the LN model but not in the LL model. In both respects the LN distribution corresponds more closely to physical reality.

Curve B in Figure 2 is a normal or gaussian curve. To transform a LN frequency curve to a gaussian frequency curve, one need only take the logarithm of the abscissa values and plot the resultant values against their normalized frequencies. Following this transformation, the full power of the techniques designed for the analysis of gaussian data, including the F-test and t-test, are available for comparing one population to another or for comparing observed distributions to theoretical models. As with a

gaussian distribution function, the LN distribution function is completely specified by just two parameters, the mean and standard deviation, or alternatively, the mean and variance.

The reproductive properties of the LN distribution follow directly from those of the gaussian distribution. If two independent gaussian variates are added the sum is a gaussian variate; consequently, if two independent LN variates are multiplied the product is an LN variate. Also, a LN variate can be multiplied by a constant or raised to a constant power and reproduce a LN variate. However, for all these cases the resulting mean and standard deviation may differ from that of the initial variates' distribution function. The reproductive properties allow the assertion that a LN distribution of asteroid diameters will lead to a LN distribution of crater diameters. The reasoning is as follows:

1. If the radii of the asteroids are LN, so are their volumes.
2. If the asteroids within the size range of interest have nearly equal densities, their masses will be nearly log-normally distributed.
3. If the velocities of the impacts are nearly uniform, or if the velocities are log-normally distributed and independently distributed with respect to the mass, then the product of powers of mass and powers of velocity will be LN. (A LN distribution of impact velocities is implied by the following traits: (a) The frequency of impacts must go to zero as the velocity of impact goes to zero. (b) Negative velocities are not allowed. (c) The velocity distribution is likely to be positively skewed, i.e. have a long tail where fewer and fewer impacts occur as velocity increases, once the value of the mode is passed).

4. Finally, if the crater diameters scale according to a law of the form

$$\text{Crater Diameter} = K_1 (\text{asteroid mass})^{K_2} \times (\text{asteroid velocity})^{K_3}$$

(Gault, 1970) where the K's are constants over the range of crater diameters of interest, one may conclude that the crater diameters should have a LN distribution.

LOG-CUMULATIVE FREQUENCY PLOT

The log-cumulative frequency plot is a graphical convenience whereon LN populations appear as straight lines. (In this study the term "population" refers to the entire range of information, zero to plus infinity, while the term "data" refers to the information in the range actually sampled. The term "transformed", preceding either "data" or "population", means that the logarithm, base 10 in this study, has been taken). Figure 3, curve A, illustrates a hypothetical LN population. The abscissa is the log of the crater diameter and the ordinate ^{IS CONSTRUCTED} such that a normal distribution will plot as a straight line. Standard works such as Abramowitz and Stegun (1972) give appropriate tables, series expansions and analytical approximations for the construction of these graphs and the subsequent analysis of the data.

Because the mean, median and mode all correspond in a gaussian distribution, the 50 percentile intercept (median) is also the mean (μ) and the mode of the transformed population. The slope of the line indicates the standard deviation of the transformed population (σ), which can be calculated as follows: Read the values at 16%, 50% and 84%, calling them v_{16} , v_{50} and v_{84} respectively. Substitute into Equation 1.

$$\sigma = 1/2(v_{84} - v_{16}) \quad (1)$$

For the hypothetical population illustrated in Figure 3, read the following values:

16 percentile - 1.32

50 percentile - 1.65

84 percentile - 1.98

Therefore, the transformed mean, mode and median are 1.65, and the standard deviation of the transformed population is at 0.33. Equation 2a gives the most numerous diameter, or the mode, of the untransformed population as 25.1. Equation 2b gives the median of the population as 44.7.

$$\text{Mode} = e^{(A_{\mu} - A^2\sigma^2)} \quad (2a)$$

$$\text{Median} = 10^{\mu} \quad (2b)$$

where $A = (n/10)$

Unfortunately, observations will always be restricted to some relatively narrow range of crater diameters, bounded by our interest, image resolution, planet size or population homogeneity. In such cases, the 50 percentile value is only the median of the transformed data; it is not the mean of the transformed data, nor the mean of the transformed population. The slope is still an indicator of the standard deviation of the transformed data, by Equation 1, though it does not indicate the standard deviation of the transformed population. Figure 3, curve B, shows the crater data of Figure 1 as it appears when plotted on log-cumulative frequency axes.

An especially useful property of the log-cumulative frequency plot is that it does not display crater density. (Crater densities and crater density differences are still important parameters, but they can be analyzed independently). Figure 4 has the same 10,000 craters that are shown in Figure 3, along with two other lines consisting of 50% and 5% of that data selected randomly. As long as the data are drawn from the same population, they will graph nearly identically. Only the probable errors associated with the mean and standard deviation of the transformed data change with the size of the data set; that is to say that the estimators of the mean and standard devia-

tion are consistent. Figure 5 is the corresponding LL version of Figure 4. The same data are in both of these figures, but the crater density differences attract the eye in Figure 5, and the fact that the samples are all drawn from the same population is difficult to see. In this artificial case, one knows the adjustment factors (x2 and x20) that would shift the 50% and 5% curves back to coincidence with the 100% curve. In practice though, if two surfaces had different crater densities, one would not know which curve to adjust nor by how much. A further benefit of analysis based on the log-cumulative frequency plots is immediately apparent: reconnaissance surveys of regional population parameters can be quickly accomplished by randomly selecting a relatively small portion of the entire crater population available and measuring and testing only those selected craters. However, one must be able to accept the larger uncertainties associated with the smaller sample sizes in order to gain a more rapid analysis.

TESTING THE ALTERNATIVE MODELS

Figure 2 illustrates that a large portion of the transformed data plots on a straight line. This strongly suggests that a LN model is appropriate. However, at small diameters the line turns downward, and off the top of this plot one would find that the line turns upward. Both of these curved segments are largely due to truncation effects associated with the 10 and 250 km diameter limits, although at least some of the deviation at the small diameters may well be due to erosion of craters with diameters less than 20 km.

In order to explain the more rigorous statistical tests that verify the log-normality of the data, we must use a mathematical model appropriate to a doubly truncated log-normal distribution.

$$\text{Let } x = \frac{\text{Log } D - \mu}{\sigma}$$

where D is the crater diameter, μ is the transformed population mean and σ is the transformed population standard deviation.

The probability that an observation, X , will be less than or equal to x is

$$\Pr_0 (X \leq x) = 1/2\pi \int_{-\infty}^x e^{-t^2/2} dt$$

if there were no truncation of the population.

Let D_1 be the minimum diameter and D_2 be the maximum diameter considered, then

$$x_1 = \frac{\text{Log } D_1 - \mu}{\sigma}$$

$$x_2 = \frac{\text{Log } D_2 - \mu}{\sigma}$$

The probability distribution function for the truncated LN distribution is then

$$\begin{aligned} \Pr(X \leq x) &= \frac{\Pr_0(X \leq x) - \Pr_0(X \leq x_1)}{\Pr_0(X \leq x_2) - \Pr_0(X \leq x_1)} \\ &= \frac{\int_{-\infty}^x e^{-t^2/2} dt - \int_{-\infty}^{x_1} e^{-t^2/2} dt}{\int_{-\infty}^{x_2} e^{-t^2/2} dt - \int_{-\infty}^{x_1} e^{-t^2/2} dt} \end{aligned} \quad (3)$$

In order to determine if the data can be satisfied by a doubly truncated log-normal model, as given in Equation 3, we must first determine values of μ and σ which are appropriate to the transformed population. Two techniques have been used to accomplish this. The simplest is devised for fitting data to doubly truncated normal distributions from knowledge of the first and second moments about the lower truncation point (Cohen, 1950). The second method is slightly more flexible and not as sensitive to non-random errors; it is a nonlinear regression by least squares on Equation 3.

In either case, once the values of μ and σ are estimated, the test of Kolmogoroff and Smirnof (Massey, 1951; Miller and Kahn, 1962) can test the data against the model. Like the chi-squared test, this is a general, non-parametric test (test results do not depend on the form of the underlying distribution function). The Kolmogoroff-Smirnof method is favored over the

chi-squared method for two reasons. First, it can provide graphical displays of confidence intervals on log-cumulative frequency plots, and second, the method is more powerful than the chi-squared test.

Figures 7 through 9 compare both the LL model, with a constant slope of -3, and the LN model, from a least squares regression, to the actual crater data. The diameter ranges 10, 20, 30, and 40 km to 250 km are treated in successive figures. Each of the models is represented by its 95% confidence bounds (i.e. data drawn from a given size-frequency distribution model, LL or LN, will have only a 5% chance of violating the appropriate bounds at any point). In every case the data are consistent with the LN model, but inconsistent with the constant slope LL model. One might hope to salvage the LL model by combining two linear segments, but, as shown in Figure 9, even the large diameters are not consistent with a line having a single slope. (A check of Figure 1 will further substantiate this). Therefore, the LL model is unsatisfactory. (Also, two linear segments allow four free parameters with which to fit the data; the LN model requires only two; thus, by Ockham's Razor alone the LN model is preferred).

The fitted values of the mean and standard deviation for the LN models differ for each of the diameter ranges shown in Figures 7 through 9. Figure 10 shows how the fitted parameters vary with minimum diameter. The predictions level out at values of $\mu = 1.363$ and $\sigma = 0.290$. A comparison of the Kolmogoroff-Smirnoff 95% confidence interval appropriate to this model against the same diameter ranges as above, shows that good agreement occurs for the 20 km and larger values of the minimum diameter, but the 10 km minimum data is inconsistent with this model.

POPULATION TIME EVOLUTION: GENERAL CONSIDERATIONS

From the end of the planetary accretion until the present, the number of cratering events per unit time has decreased, probably more or less monotonically. But is it possible that the population parameters of the impacting

bodies have also changed? It can be assumed that as asteroid-asteroid collisions continuously occur, the mean radius of the population would continuously decrease (independent of the form of the underlying size-frequency distribution). The standard deviation would generally increase with time. Unfortunately, Mars is not the ideal locality to search for these time variations because of the action of size-dependent erosive and obliterative processes. Nonetheless, on Kolmogoroff's hypothesis the development of a log-normal asteroid size-frequency distribution is coupled to such a time evolution. Neukum et al. (1975) attempted to observe evolution effects but was unsuccessful. Because their negative result poses a significant threat to a LN model, I feel a critical review is necessary.

The data base of Neukum et al. consisted of small craters from selected lunar regions. However, their data covered different size ranges in different study regions, and to establish a "calibration curve", virtually all of their data required an adjustment in terms of crater density. This required averaging densities where the diameter ranges overlapped, in order to determine an adjustment factor. The process of averaging diminishes the possibility of recognizing population variations, especially on log-log axes. Their averaging scheme was not successful; it left the crater density at any diameter in doubt by approximately $\pm 50\%$, due to a persistent trend in their data, regardless of size range, to display a shallower slope at the larger diameter extreme than at the smaller diameter extreme. The averaging, therefore, commonly occurred between two segments having different slopes - leading to a large probable error in the adjustment factor. Although Neukum et al. (1975) were careful to remove suspected secondary craters from their counts, the tendency of the small craters to lie on a slope approaching -4 may indicate that many secondaries went unrecognized. In fact, their calibration curve looks strikingly like the lunar curve for secondaries plus primaries presented by Shoemaker (1965, Figure 47). Neither their data nor their technique was truly suitable to the search for time dependence and they found none.

For the reasons mentioned previously, a Mars-based data set offers little more hope of uncovering time dependence, and, indeed, I found no irrefutable cases. But finding likely regions to examine for time dependent effects or for abnormal erosional effects (treated in the next section) employs the same technique which is introduced here. The method uses a LN model with a μ and a σ appropriate to the planetwide population and searches out regions that violate the corresponding Kolmogoroff-Smirnoff bounds. To accomplish this end, each $5^\circ \times 5^\circ$ square was tested in succession. Commonly, a single square contained an insufficient ^{number} of craters to warrant testing; however, when combined with enough neighboring squares, a meaningful test was possible. Therefore, the procedure employed requires a minimum number of craters per test (minimum statistical resolution) and allows free adjustment of the surface resolution. Figures 11 through 14 display some of the results of this procedure. When a violation of the limits occurred, the computer placed a dot in the center of the square where the analysis was initiated, and drew a box around the area included in the statistical test. As explained in the figure captions, one can display areas violating either the upper or the lower bounds over any crater diameter range and at any confidence level. The meandering lines in these figures (modified after Carr, et al., 1973) separate the plains units (predominantly of volcanic origin) from the cratered units. The Roman Numerals used in the remainder of the paper will refer to the regions designated on Figures 11 through 14.

Having located the abnormal regions, comparison of their data by non-parametrical techniques can proceed. The method for comparing the data mean values is Fisher's randomization test as described by Snedecor and Cochran (1973). Comparison of the data standard deviations is with the Miller Jackknife test as described by Hollander and Wolf (1973).

Indications of possible time variations come from Figure 10. Below 25 km the fitted value of the mean decreases (and the standard deviations increase) as successively smaller crater diameters are included, demonstrating that the population parameters appropriate to those craters greater than 25 km will not suffice upon inclusion of diameters less than 15 km. Because the cratered southern hemisphere greatly dominates these statistics, and there obliteration of the small craters presumably proceeds more rapidly than that of the large ones, the small craters have a lesser mean age than do the large craters (Hartmann, 1971). Being more recent, the small craters should represent a population with a smaller mean value; this is consistent with the above observations and consistent with a time dependence of population parameters.

Further arguments for a time evolution appear in a later section on the analyses of abnormal Region II (Figures 11 and 12) which shows an overabundance of small craters and is a relatively youthful surface.

REGIONAL CRATER OBLITERATION

Two general classes of crater oblitative processes must be considered: those that remove craters with rates directly related to crater diameter and those with rates inversely related to crater diameter. Processes in the latter class are more numerous, and include most types of sedimentary filling and magmatic inundation. These processes undoubtedly dominate the former class in terms of the total effect on the crater population. Even so, their effects seem mainly confined to the less than 15 km diameter range, as inferred from Figure 10 which shows that above approximately 15 km minimum diameter, a single set of population parameters suffices to describe all larger diameter data sets. Furthermore, because a log-normal model fits even the 10-250 km data set, crater obliteration at the small diameters is probably not as extensive as studies using a LL model had indicated (e.g. K. C. Jones, 1974, Hartmann, 1973).

Locally, a relatively extensive obliteration of small craters will lead to a violation of the lower Kolmogoroff-Smirnoff bounds. Figures 13 and 14 show just such areas: Regions IV, V, VI, VIII, IX, XII and XIII.

Regions associated with the cratered southern terrains and with a relative overabundance of small craters command particular interest. If substantial ice exists anywhere in the martian subsurface, it may result in the more rapid isostatic adjustment of craters than in regions devoid of subsurface ice. Isostatic adjustment is probably the main process with a rate related directly to diameter and capable of affecting substantial surface area. In Figures 11 and 12 two such regions appear: Regions VII and XI.

The other regions not yet mentioned are Region X, the Chryse basin, where the Viking softlander is to touch down; Region II, including most of the volcanic plains of the northern hemisphere; and Region III, including the volcanic plains of Hesperia Planum. Region I is utilized as a reference surface and does not appear on Figures 11 through 14.

A discussion of each of these thirteen regions now follows. The geologic descriptions of each region are from Carr, et al. (1973). Topographic information is from Christensen (1975), and the isostatic states are from Phillips and Saunders (1975); these sources should be consulted for additional descriptions and details.

REGION I

Region I is defined to be the area south of the boundary between the cratered units and plains units and north of -30° latitude. This region is not an abnormal region, but a region against which to compare the abnormal regions. It consists almost uniformly of heavily cratered units, with the exception of Hesperia Planum. In order to avoid the eolian blanketed terrains

mapped by Soderblom, et al. (1974), only terrain north of -30° latitude was included. However, Region I contains significant portions of abnormal Regions II, VII, VIII, IX, and XIII; but Region I's data mean value is 1.371 and standard deviation is 0.244 compared with values of 1.386 and 0.244 for the entirety of the cratered units. The difference in the mean values is not significant at the 90% confidence level.

Region I appears to be as good a touchstone for comparative analysis as available in the martian southern hemisphere.

REGION II

Region II is the largest contiguous anomalous region identified on Mars, covering most of the surface north of the boundary between the cratered units and plains units. Although this region extends south of the boundary in some localities, for the purposes of this study only that portion lying north of the boundary constitutes Region II.

The geologic units of Region II are all lightly cratered and, therefore, relatively young. The units are of mixed origin, with volcanic and eolian deposits. The range of altitude in this region exceeds that of any other region studied, reaching from -2 km north of the crater Mie to +28 km atop Olympus Mons. However, most of Region II lies at moderate altitudes on relatively shallow regional slopes.

Region II consists of a nearly homogeneous crater population. To check for anomalous regions within Region II, the data from this region alone were fitted to a LN model, and subregions violating the Kolmogoroff-Smirnoff bounds for that model were sought. The results appear in Figure 15. Areas around the volcanic cones show a significant excess of small craters compared to the rest of Region II. This may be attributable to many local endogenetic calderas

or to significant age differences. A similar test for an excess of large craters revealed that north of the boundary between the cratered units and plains units, only Region VI has a significant excess of large craters.

Region II, considered as a whole, derives its anomalous nature from an overabundance of small craters with respect to the planetwide average. The region is well defined in the 10 and 25 to 250 km diameter range anomaly maps (Figures 11 and 12). Erosion of craters and time evolution of impactors causes this persistent overabundance of small craters. The erosion is not manifested in Region II; a relative lack of erosion there compared with the southern hemisphere causes the excess of small craters observed in Region II.

Some evidence supporting the time evolution of impacting bodies has already appeared earlier in this study. The examination of Region II adds two more lines of evidence: (1) Erosional effects, planetwide, are inappreciable above 15 km diameter (see arguments at the beginning of this section); yet Region II continues to register a crater anomaly in the range 25-250 km diameter (Figure 12). Erosion alone, therefore, will not explain the anomalous behavior of Region II. However, one expects this apparent overabundance of small craters in all diameter ranges if the mean diameter of the impacting bodies has decreased with time. (2) The Region I population parameters for the range 10-250 km diameter are $\mu = 1.228$ and $\sigma = 0.335$ where those for Region II are $\mu = 0.975$ and $\sigma = 0.381$. Therefore, 80% and 50% respectively of the fitted populations lie in the diameter range 10-250 km. Therefore, to go from a Region II population to a Region I population requires removal of at least 40% of the small craters. This much (minimum) obliteration is impossible to confine to the 10-15 km diameter range; the simpler alternative of time dependent population parameters is favored.

Region III

Region III essentially coincides with Hesperia Planum, and like much of Region II this region consists of volcanic plains. The crater anomaly maps in Figures 11 and 12 illustrate the close kinship of these two regions, and a separate discussion of Region III will not be undertaken. The observations and arguments pertinent to Region II also pertain to Region III without significant alternation.

REGIONS IV AND V

These two regions, IV and V, are considered together because of their similarity in geologic and geographic setting, crater densities, and data mean values and standard deviations. Both regions lie south of -30° latitude in the mantled terrains of the cratered units (except where Region V breaks into Hellas Planitia, which, from a lack of craters there, is statistically insignificant).

A dearth of small craters up to 20 km diameter characterizes these regions on Figures 13 and 14. (Intermediate diameter range anomaly maps confirm the persistence of these regions). Although Soderblom et al. (1974) did not find much evidence for mantling of craters with diameters greater than 10 km, the effects are present. The favored interpretation of these and intermediate crater anomaly maps is that severe eolian sedimentation has affected all of Regions IV and V to beyond a diameter of 10 km, and that in some locales the blanketing is of importance to beyond 20 km diameter.

Recent local disturbances caused the gaps between these two regions. The gap at 25° West longitude has suffered the effects of the Hellas event, which raised high mountains and ejected considerable debris, undoubtedly obliterating large and small craters alike. Similar arguments pertain to the formation of the Argyre basin and the gaps which surround it.

REGION VI

Region VI lies immediately to the north of the northernmost extent of the cratered units. It consists of plains units and knobby terrain. The imagery in this area is among the poorest obtained anywhere on Mars; therefore, conclusions concerning Region VI are necessarily tentative and correspondingly brief.

The crater anomaly maps (Figures 13 and 14) for Region IV reveal an apparent depletion of craters in the diameter range 10 to 15 km. Because this region is in the northern mantled terrains, the small craters could have been inundated with dust. This conclusion remains tentative because of the poor quality of the available data; perhaps image resolution alone could be blamed for the anomaly.

REGIONS VII AND VIII

Astride the border between the cratered units and plains units, southeast of Acidalum Planitia, lie Regions VII and VIII. These two regions are discussed together because they hold a large portion of their areas in common. These regions possess no unusual geology. The area is rather flat and in isostatic equilibrium. The crater density in this area, however, is below that of Region I by 9 standard deviations in the 10-250 km diameter range. (This is calculated with the portion of Region VII lying north of the boundary between the cratered units and plains units excluded; even larger differences result if this northern portion is included).

The crater statistics of this area are extremely complex. Briefly, from Figures 11 through 14 and intermediate diameter range maps, Region VIII shows a relative depletion of small craters (mostly in the range 10 to 20 km diameter). This is a very severe depletion, judging from the 9σ crater density difference with Region I. In addition, Region VII indicates that the northwest portion of Region VIII also has a relative overabundance of craters in the mid-diameter

ranges (20 to >25 km) with respect to the large craters. Even so, the absolute crater densities are low in the midrange of diameters (at the 95% confidence level) when compared to Region I.

The proposed explanation of these observations requires either crater obliteration at all diameters, but with greatest efficiency for the smallest and largest diameter extremes, or complete obliteration of all craters with subsequent obliteration of the largest and smallest diameters of the newly formed population. No single erosive process can meet these requirements. Because Sagan et al. (1973) found few wind streaks in this area, much eolian sedimentation is unlikely; an interpretation consistent with Soderblom's et al. (1974) observation of a lack of mantling of the small craters there. More likely, most of the small craters have suffered magmatic inundation. A few examples of what appear as breached crater walls (e.g. the crater Gill and the small crater north of it) lend support to this interpretation.

The agent responsible for the obliteration of the large craters is of great interest. The difference between this area's large-crater population and that of Region I implies that approximately 10% of the craters greater than 25 km have been erased. A real possibility exists that this fraction of craters has drowned in eruptions emanating from their own floors or nearby sources. But the proximity of this area to the knobby terrain (immediately to the north-east) fuels an alternative explanation: the large craters have undergone rapid isostatic rebound due to the presence of subsurface ice. Both Sharp (1973) and Milton (1973) argue that the knobby terrain may have resulted from the presence of subsurface ice.

The coupling of an active volcanic province with subsurface ice is not impossible. The transition of this area from a cold to a thermally active province could have caused the collapse into knobby terrain and the very rapid isostatic rebound of large craters.

REGION IX

Region IX lies just east of Region VIII and entirely within cratered units. It rests on a north-facing slope spanning a 2 to 5 km altitude range.

Figures 12 and 13 show Region IX to have a marked deficiency of small craters. This trend is more firmly established in Region IX than in any other region found on Mars, maintaining the deficiency to beyond 25 km diameter.

The cause for such a pronounced anomaly is unknown but the proximity of this region to Region VIII strongly suggests that magmatic inundation could be the active agent here as well.

REGION X

Region X lies adjacent to, though not conterminous with, Region II. It is predominantly north of the boundary between the cratered units and plains units and contains the basin of Chryse Planitia. As in Region II, Region X consists primarily of plains units, although it also includes some chaotic and cratered terrains in its southern and eastern extents. Topographically, Region X lies mostly within a basin which descends to 3 km below the adjacent cratered terrains. The Chryse basin exhibits a negative isostatic anomaly suggesting the presence of a thick, low density unit. Channels connect the basin with the adjacent chaotic terrains, although flow direction indicators are ambiguous.

Region X differs from its neighbor, Region II, in at least one major statistical feature: in Region X the anomaly appears only on the 10-250 km anomaly map (Figure 11), it is not present on a 15-250 km anomaly map, whereas Region II's anomalistic behavior extends to the large diameter ranges. However, a complete absence of large craters in the basin has caused a considerable loss of ground resolution, and thus the adjacent normal terrains were automatically incorporated in these statistical tests. This incorporation obscures any anomalistic population within the basin.

The similarity of the crater populations of Regions X and II requires only that both regions be erased of all craters at approximately the same time and then be left to start accumulating craters anew. Thus, the formation of Chryse basin must be contemporaneous with or predate the general obliteration episode which affected the entire northern plains. Two plausible processes could have delivered sediments to the basin, obliterated the craters, and caused the negative anomaly: (1) eolian transport from the North, and (2) aqueous transport from the South and West.

Although Soderblom et al. (1974) did not include Chryse basin within their mantled terrains, Sagan et al. (1973) mapped strong wind direction indicators coming from the Northeast, off Acidalius Planitia and the mantled terrains. Thus at least some craters may have suffered obliteration by eolian deposition.

The existence of aqueous agents is more problematical. If the chaotic terrains have resulted from the collapse of overlying sediments after the withdrawal of subsurface ice, then any liquid produced would have come down into the basin (assuming conditions were correct for melting rather than for sublimation of the ice). This could explain the channels connecting the basin and the chaotic terrains.

Whether one or both of these plausible erosional agents actually occurred, the crater population in Region X indicates that a major episode of obliteration there and in Region II were roughly coincident in time.

REGION XI

Region XI is a small region lying northeast of Argyre basin in cratered terrains of normal appearance. It rests on a shallow slope facing the basin and elevated above the basin floor by approximately 3 km.

Although Region XI's crater size-frequency distribution is interesting from the standpoint of subsurface ice, its small areal extent poses major problems. The crater anomaly there may simply be a coincidental grouping of craters;

even if it is not, the data set and surface area are small and not readily amenable to detailed analysis.

At the 90% confidence level no differences in the data mean values or standard deviations for the size range 10-25 km exist between Region XI and I. In the diameter range 25-250 km, however, the mean value of Region XI is less than that of Region I at the 99% confidence level. This is consistent with abnormally rapid isostatic rebound and concomitant obliteration of the largest craters. Unfortunately, the region is sparse in morphologies generally considered as indicators of possible sites of subsurface ice. Thus, the likelihood of subsurface ice in Region XI remains poorly assessed.

REGIONS XII AND XIII

Regions XII and XIII are presented only for the sake of completeness. Both of these regions seem to be statistical quirks rather than meaningful anomalies. These regions show a depletion of craters in the midrange diameters (20 to 30 km) only. A rather complex geological history would need to be constructed, with superpositioning of two or more obliterative processes, in order to explain the observed anomalies. With the requisite superpositioning of processes, at least one process would be expected to have also affected the craters adjoining these regions. Therefore, regions with different types of anomalies would border Regions XII and XIII. Because no such "paired" anomalies are found, the favored explanation is that of statistical coincidence.

CONCLUSIONS

To analyze a crater population that results from an integration of a time dependent impacting population is a difficult task. Added complications arise because different diameter ranges may be under the dominion of different physical processes and are, therefore, likely to possess different distribution parameters or even different distribution functions. By restricting the range of crater

diameters and by considering only the extreme wing of the size-frequency distribution, some gains have been made in obtaining the form of the distribution law. A linear relationship between the log of the crater diameters and the log of the crater densities is a less satisfactory representation than is a log-normal law, as judged by formal statistical inference.

Twelve regions differ significantly from the planetwide crater population average. Simple processes of sedimentation suffice to explain most of the observations, but some evidence for subsurface ice, and time evolution of the impacting bodies also exists.

Replacing a LL law by a LN law calls into question a great portion of the previously held conclusions. The impact is greatest on those studies reporting absolute dates derived from the density of small craters. The parallel, straight isochrons of the LL model must be replaced by arching nonparallel lines. Dating based on smaller craters may have systematically underestimated ages by more than an order of magnitude. The absolute ages were already poorly determined because of the difficulty of estimating impact rates, but the errors caused by application of an incorrect model are in addition to any previously acknowledged uncertainties.

The relation between a breccia process and the observed crater size-frequency distribution bears on the origin and nature of the impacting bodies. Two possible populations present themselves: early stray bodies in nearly circular orbits and asteroids in more eccentric orbits. Both of these populations probably once contained a sufficient density of bodies to facilitate abundant mutual collisions. Unfortunately, these two possible populations each carry separate forecasts for the success of interplanetary time correlation. If cratering was primarily caused by bodies in low eccentricity orbits, then neither the crater density nor the population parameters must correlate between planets.

However, if the cratering was primarily caused by bodies in high eccentricity orbits, then the population parameters, and perhaps the crater densities, should correlate between planets.

The analyses of this study do not exhaust the possibilities of crater population studies on Mars, but they do illustrate the use of new and more rigorous analytical techniques applicable not only to Mars, but to all cratered bodies.

Acknowledgments. This paper represents a portion of the work done for the author's Ph.D. thesis (Harvard University, 1975) and reflects the aid and guidance of many individuals. I am particularly grateful to R. M. Goody and R. J. O'Connell who were my principal advisors and to J. P. Watt who supplied the nonlinear regression program.

The research for this paper was supported by NASA Grant NGL 22-007-228.

REFERENCES

- Abremowitz, M., and Stegun, I. A., eds., *Handbook of Mathematical Functions*, Dover Publications, Inc., New York, 1972.
- Aitchison, S., and Brown, J. A. C., *The Lognormal Distribution*, Cambridge University Press, 1973.
- Carr, M. H., Masursky, H., and Saunders, R. S., A generalized geologic map of Mars, *J. Geophys. Res.*, 78, 4031, 1973.
- Christensen, E. S., Martian topography derived from occultation, radar, spectral, and optical measurements, *J. Geophys. Res.*, 80, 2909, 1975.
- Cohen, A. C., Jr., Estimating the mean and variance of normal populations from singly truncated and doubly truncated samples, *Ann. Math. Stat.*, 21, 557, 1950.
- Epstein, B., The mathematical description of certain breakage mechanisms leading to ^{the} logarithmico-normal distribution, *J. Franklin Inst.*, 224, 471, 1947.
- Gault, D. E., Saturation and equilibrium conditions for impact cratering on the lunar surface: criteria and implications, *Radio Sci.*, 5, 273, 1970.
- Hartmann, W. K., Martian cratering II. Theory of crater obliteration, *Icarus*, 16, 410, 1971.
- Hartmann, W. K., Martian cratering 4. Mariner 9 initial analysis of crater chronology, *J. Geophys. Res.*, 78, 4096, 1973.
- Hollander, M., and Wolfe, D. A., *Nonparametric Statistical Methods*, Wiley & Sons, 1973.
- Jones, J., The mass distribution of meteoroids and asteroids. *Canadian J. Phys.*, 46, 1101, 1968.
- Jones, K. L., Evidence for an episode of crater obliteration intermediate in Martian history, *J. Geophys. Res.*, 79, 3917, 1974.
- Kolmogoroff, A. N., Über das logarithmisch normale verteilungsgesetz der dimensionen der teilchen bei zerstückelung, *Doklady*, 31, 99, 1941.
- MacDonald, T. L., Studies in lunar statistics, *J. British Astron. Assoc.*, 41, 288, 1931.
- Massey, F. J., Jr., The Kolmogorov-Smirnov test for goodness of fit, *J. Amer. Statist. Assoc.*, 46, 68, 1951.
- Miller, R. L., and Kahn, J. S., *Statistical Analysis in the Geological Sciences*, Wiley & Sons, 1962.

- Hilton, D. J., Water and processes of degradation in the Martian landscape, *J. Geophys. Res.*, 78, 4037, 1973.
- Neukum, G., König, B., and Arkani-Hamed, A., A study of lunar impact crater size-distributions, *The Moon*, 12, 201, 1975.
- Phillips, R. J., and Saunders, R. S., The Isostatic state of Martian topography, *J. Geophys. Res.*, 80, 2893, 1975.
- Piotrowski, S., The collisions of asteroids, *Acta Astronautica*, Series A, 5, 115, 1953.
- Razumovsky, N. K., Distribution of metal values in ore deposits, *Doklady*, 18, 814, 1940.
- Sagan, C., Veverka, J., Fox, P., Dubish, R., Frency, R., Gierasch, P., Quam, L., Lederberg, J., Levinthal, E., Tucker, R., and Eross, B., Variable features on Mars, 2, Mariner 9 global results, *J. Geophys. Res.*, 78, 4163, 1973.
- Sharp, R. P., Mars: fretted and chaotic terrains, *J. Geophys. Res.*, 78, 4073, 1973.
- Shoemaker, E. M., Ranger VII. Part II, Experimenters' analyses and interpretations, *JPL Technical Report No. 32-700*, 1965.
- Sjogren, W. C., Lorell, J., Wong, C., and Downs, W., Mars gravity field based on a short-arc technique, *J. Geophys. Res.*, 80, 2899, 1975.
- Snedecor, G. W., and Cochran, W. G., *Statistical Methods*, Iowa State University Press, 1973.

FIGURE CAPTIONS

- Figure 1: The crater data (10-250 km diameter) used in this paper as they appears when plotted on log-log axes in a manner analogous to that suggested by K. L. Jones (1974). In comparison to the line of -3 slope, the data are gently, but continuously, bending.
- Figure 2: The log-normal frequency curve (A) can be transformed to a gaussian frequency curve (B) by plotting the log of the diameter against the normalized frequency. The positive skewness of the log-normal curve results in the successive rightward shift of the median and mean away from the mode.
- Figure 3: The crater data (10-250 km diameter) as in Figure 1, but plotted on log-cumulative frequency axes. The long linear segment suggests the applicability of a log-normal size-frequency distribution model for large martian craters. A numerical example in the text utilizes the hypothetical population lines.
- Figure 4: The three curves represent 100%, or all 10,000 craters, and 50% and 5% selected at random from the total data set. Because crater densities are not displayed on a log-cumulative frequency plot, the fact that all three data sets were drawn from the same population is immediately apparent. These data sets are repeated on log-log axes in Figure 5.
- Figure 5: The three curves represent 100%, or all 10,000 craters, and 50% and 5% selected at random from the total. Crater density differences are apparent, but the fact that all three data sets are drawn from the same population is difficult to recognize. These same three data sets are on log-cumulative frequency axes in Figure 4.

- Figure 6: The Kolmogoroff-Smirnoff 95% confidence limits appropriate to a log-log distribution model (with a constant slope of -3) and a log-normal distribution model (with $\mu = 1.228$ and $\sigma = 0.335$ as determined by a least squares fit to the 10-250 km diameter data) compared to the crater data over the range 10-250 km diameter. The LN model provides a good fit to the data but the LL model does not.
- Figure 7: The Kolmogoroff-Smirnoff 95% confidence limits appropriate to a log-log distribution model (with a constant slope of -3) and a log-normal distribution model (with $\mu = 1.317$ and $\sigma = 0.304$ as determined by a least squares fit to the 20-250 km diameter data) compared to the crater data over the range 20-250 km diameter. The LN model provides a good fit to the data but the LL model does not.
- Figure 8: The Kolmogoroff-Smirnoff 95% confidence limits appropriate to a log-log distribution model (with a constant slope of -3) and a log-normal distribution model (with $\mu = 1.365$ and $\sigma = 0.289$ as determined from a least squares fit to the 30-250 km diameter data) compared to the data over the range 30-250 km diameter. The LN model provides a good fit to the data but the LL model does not (note violation of the upper portion of the data curve).
- Figure 9: The Kolmogoroff-Smirnoff 95% confidence limits appropriate to a log-log distribution model (with constant slope of -3) and a log-normal distribution model (with $\mu = 1.309$ and $\sigma = 0.304$ as determined by a least squares fit to the 40-250 km diameter data) compared to the data over the range 40-250 km diameter. The LN model provides a good fit to the data, but the LL model does not.

Figure 10: The population parameters, mean and standard deviation, obtained by fitting the data to a log-normal model, graphed as a function of minimum diameter (holding the maximum diameter fixed at 250 km). The two methods used in the fitting (described in text) agree very well above approximately 20 km minimum diameter at which point the curves also nearly level out.

Figure 11: Regions on Mars found to violate the upper bounds of a 90% Kolmogoroff-Smirnoff confidence interval appropriate to a log-normal model with $\mu = 1.228$ and $\sigma = 0.335$ when craters in the range 10-250 km diameter are examined (10 or more craters per analysis). Vastitas Borealis and Hesperia Planum have an excess of small craters.

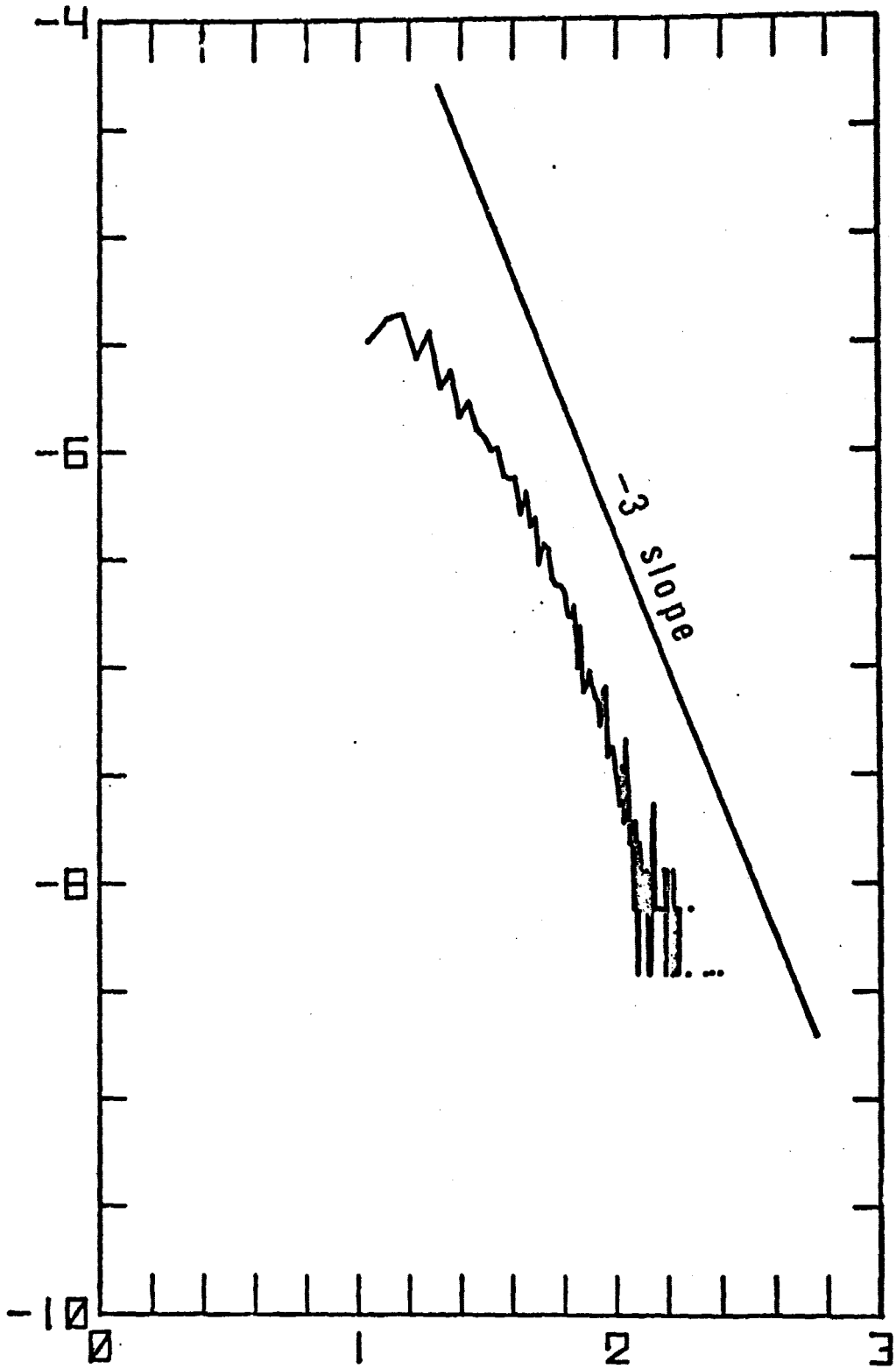
Figure 12: Regions on Mars found to violate the upper bounds of a 95% Kolmogoroff-Smirnoff confidence interval appropriate to a log-normal model with $\mu = 1.363$ and $\sigma = 0.290$ when craters in the range 25-250 km diameter are examined (10 or more craters per analysis). Several regions show an excess of small craters.

Figure 13: Regions on Mars found to violate the lower bounds of a 90% Kolmogoroff-Smirnoff confidence interval appropriate to a log-normal model with $\mu = 1.228$ and $\sigma = 0.335$ when craters in the range 10-250 km diameter are examined (10 or more craters per analysis). Several regions show an insufficiency of small craters.

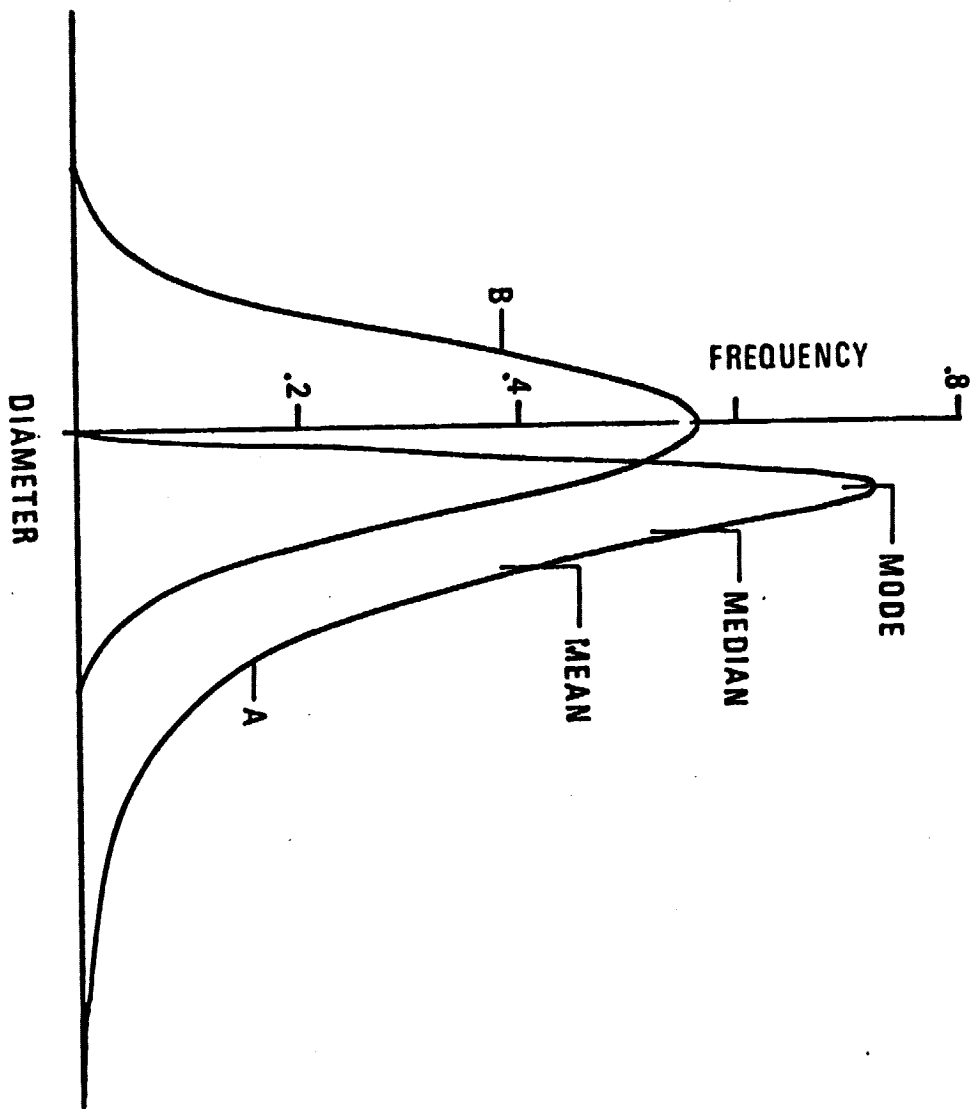
Figure 14: Regions on Mars found to violate the lower bounds of a 95% Kolmogoroff-Smirnoff confidence interval appropriate to a log-normal model with $\mu = 1.316$ and $\sigma = 0.305$ when craters in the range 20-250 km diameter are examined (10 or more craters per analysis). Several regions show an insufficiency of small craters.

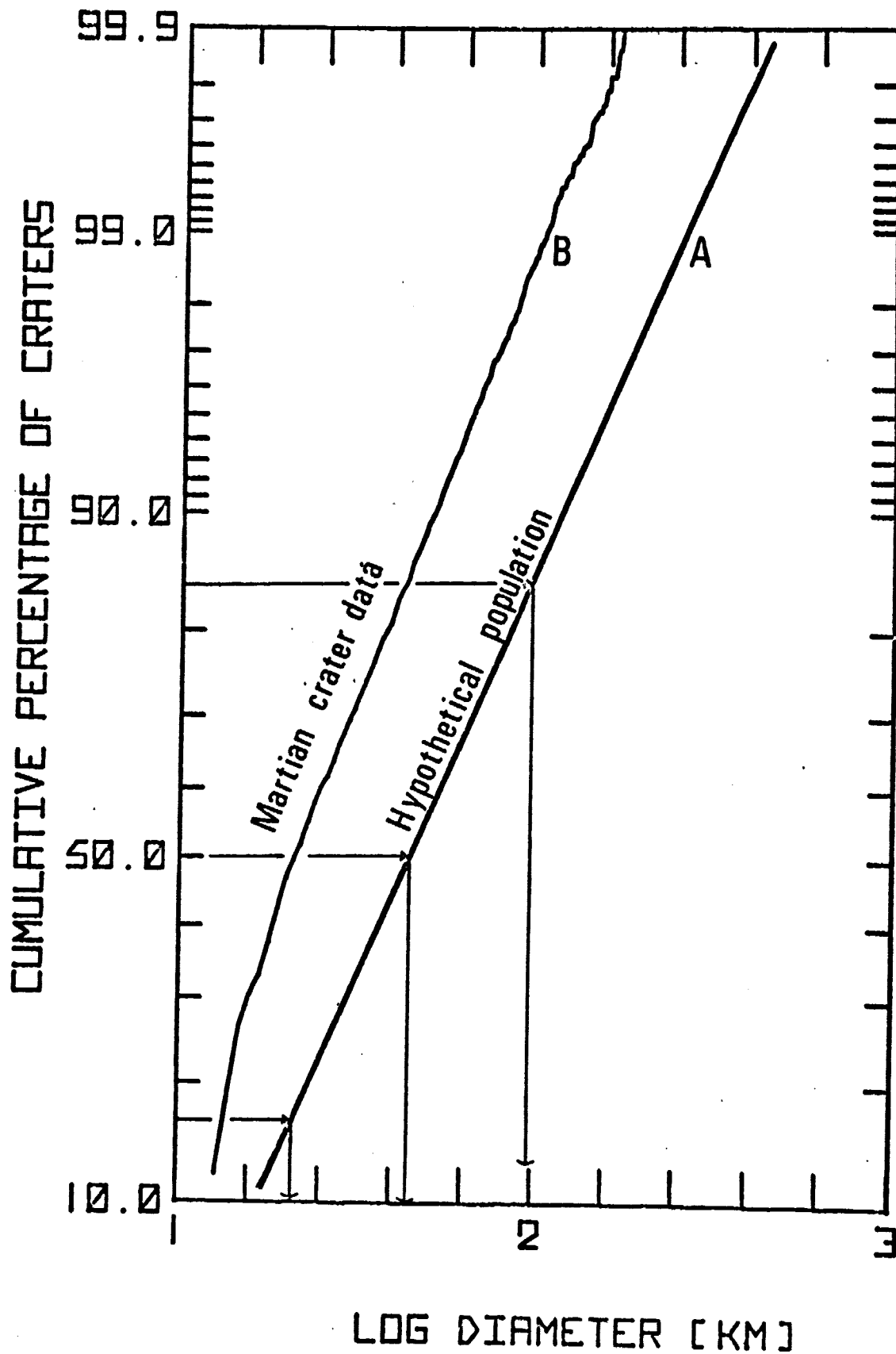
Figure 15: Regions on Mars found to violate the upper bounds of a 95% Kolmogoroff-Smirnoff confidence interval appropriate for a log-normal model with $\mu = 0.957$ and $\sigma = 0.381$ when craters in the diameter range 10-250 km are examined (8 or more craters per analysis). The values of μ and σ were obtained by a least-squares fit to the data of Region II. Areas surrounding the large volcanic cones show an excess of small craters.

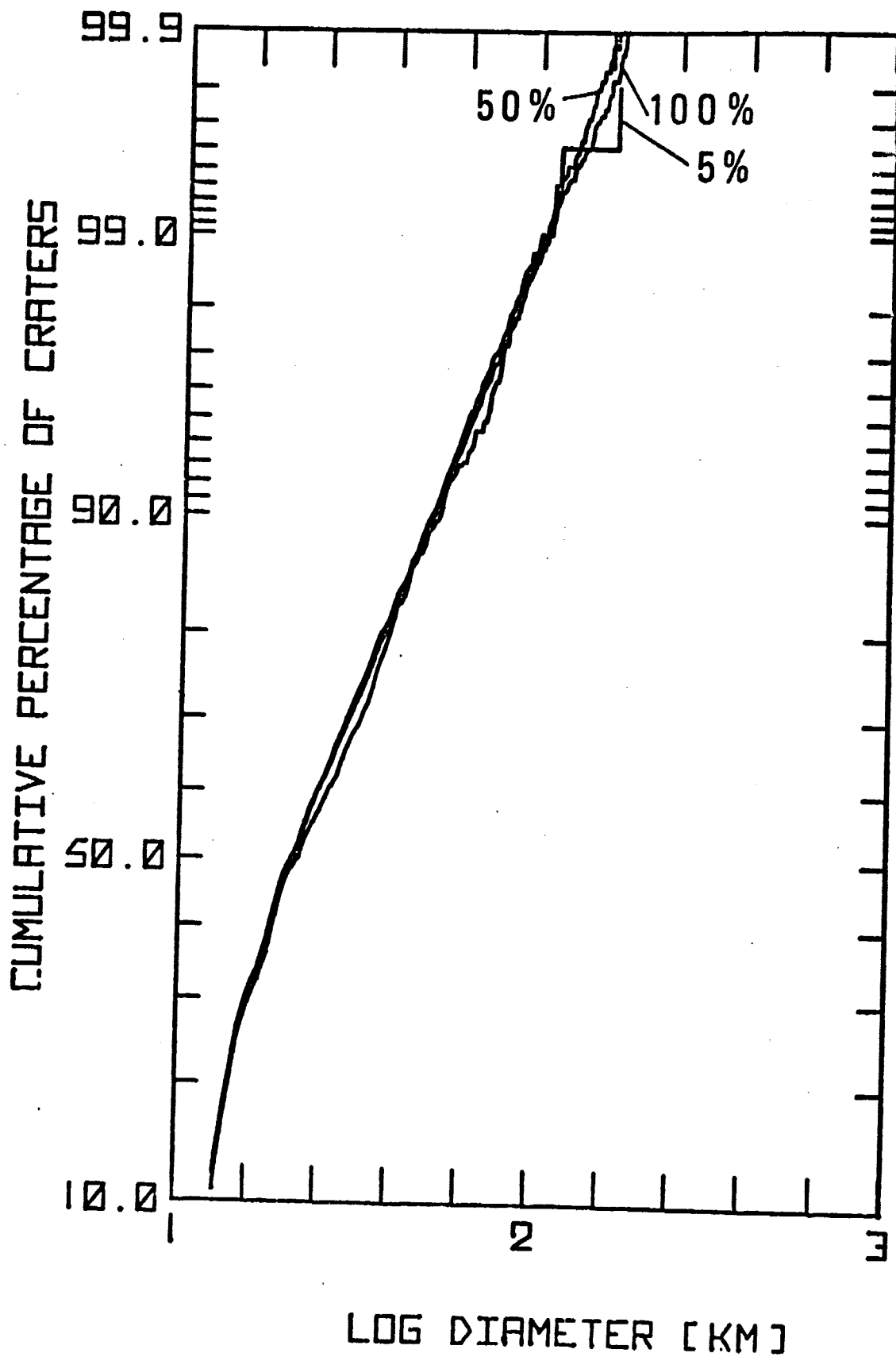
LOG CRATER FREQUENCY PER 50 KM



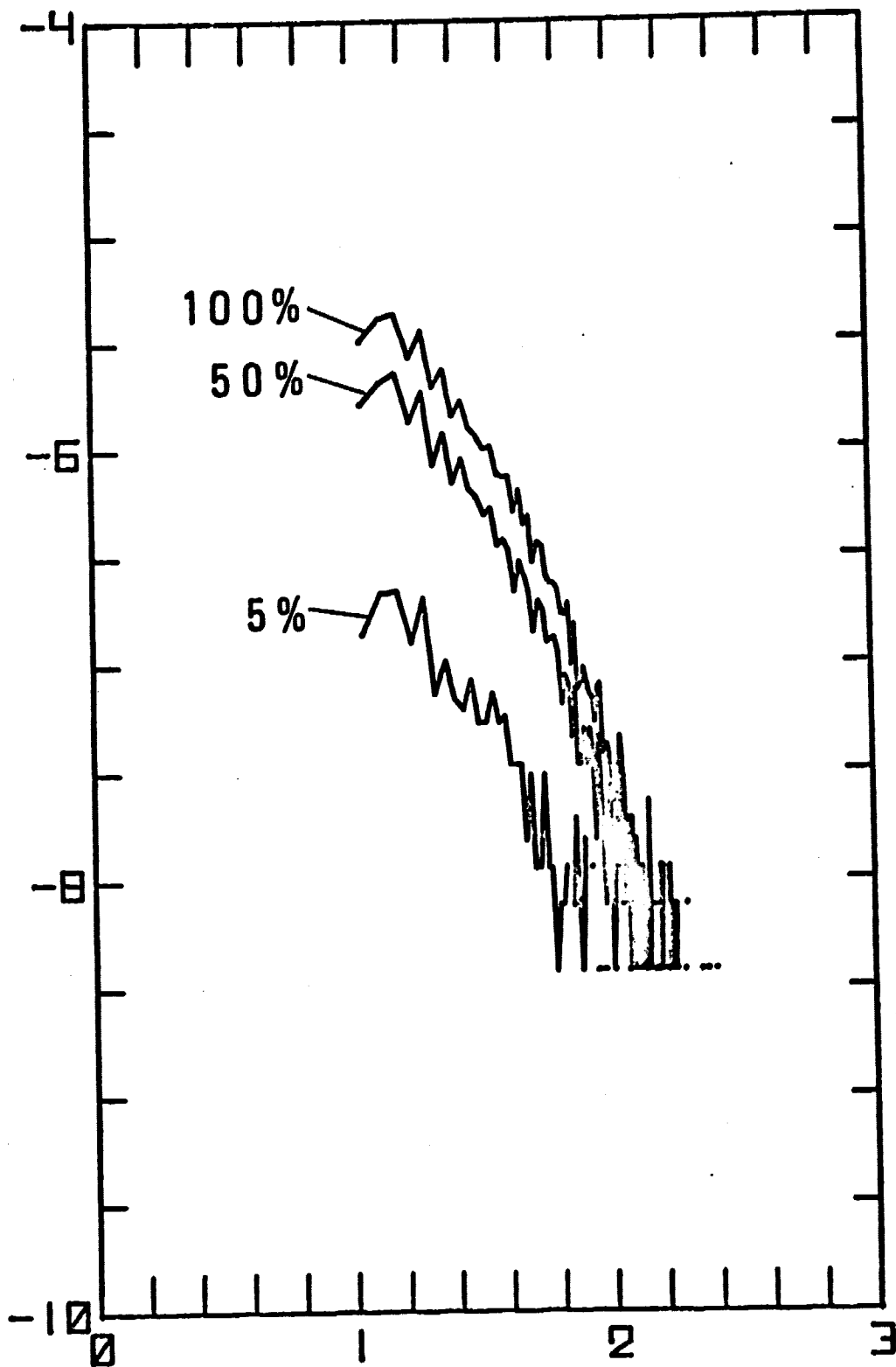
LOG DIAMETER [KM]

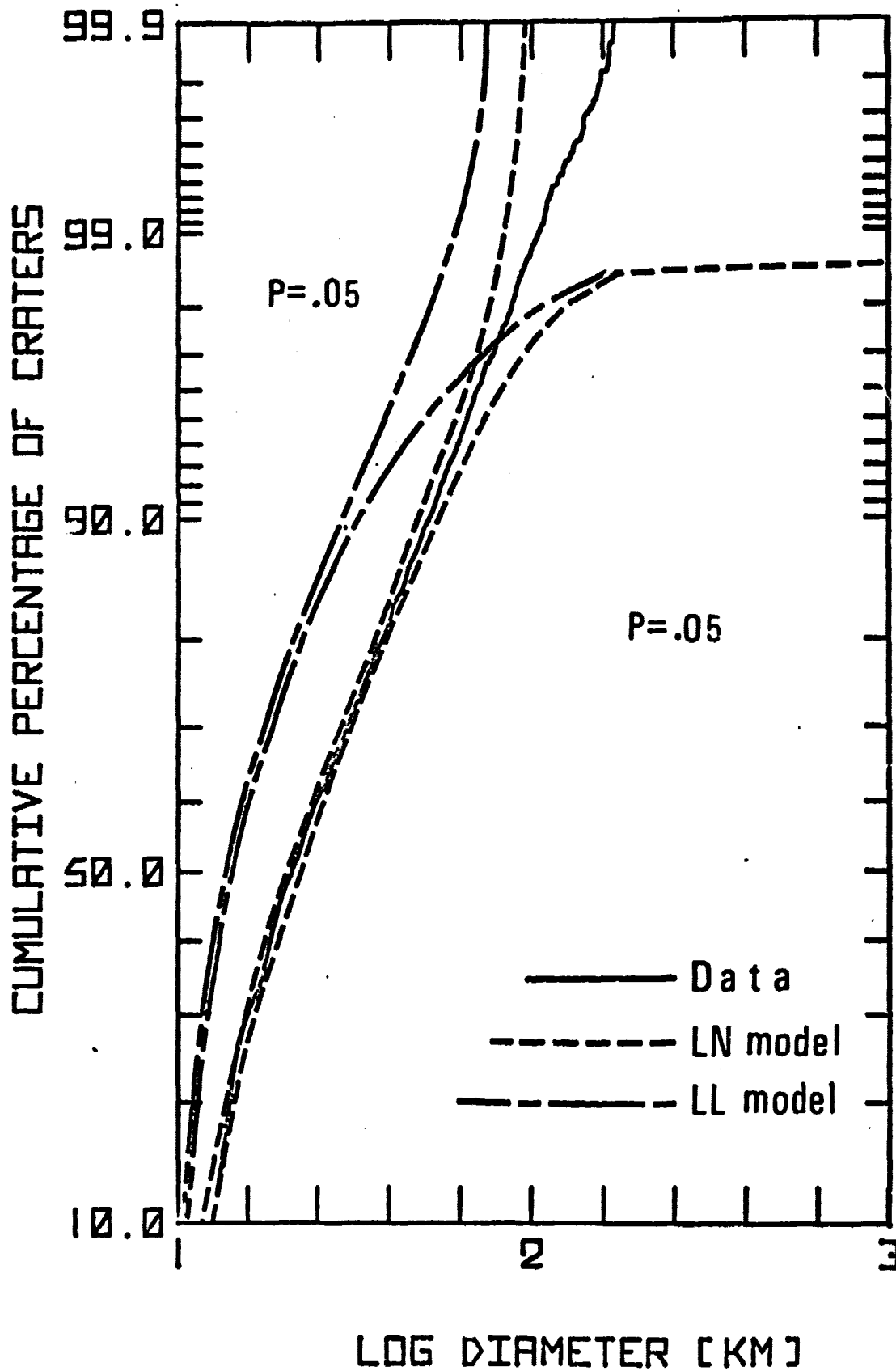


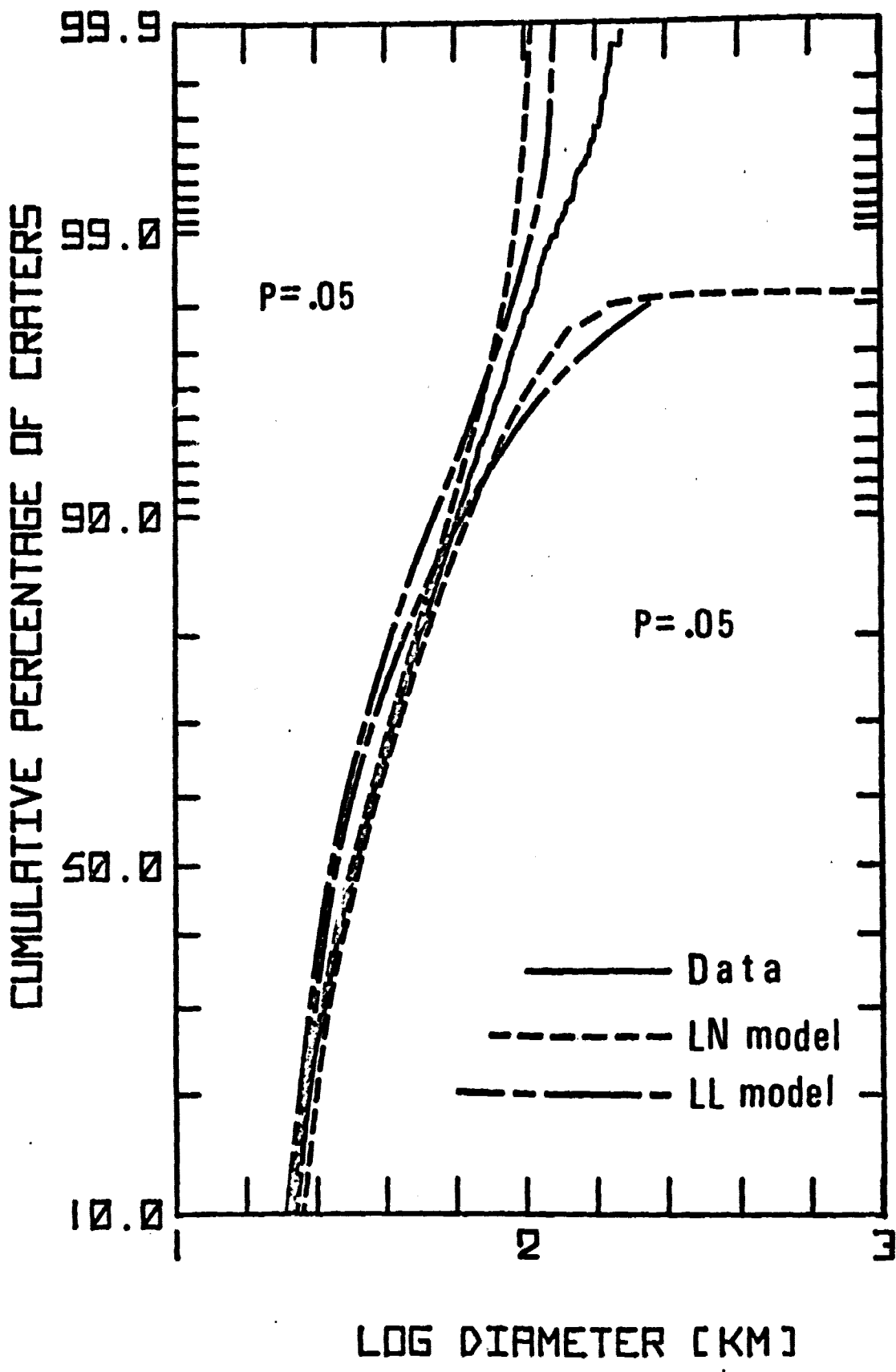


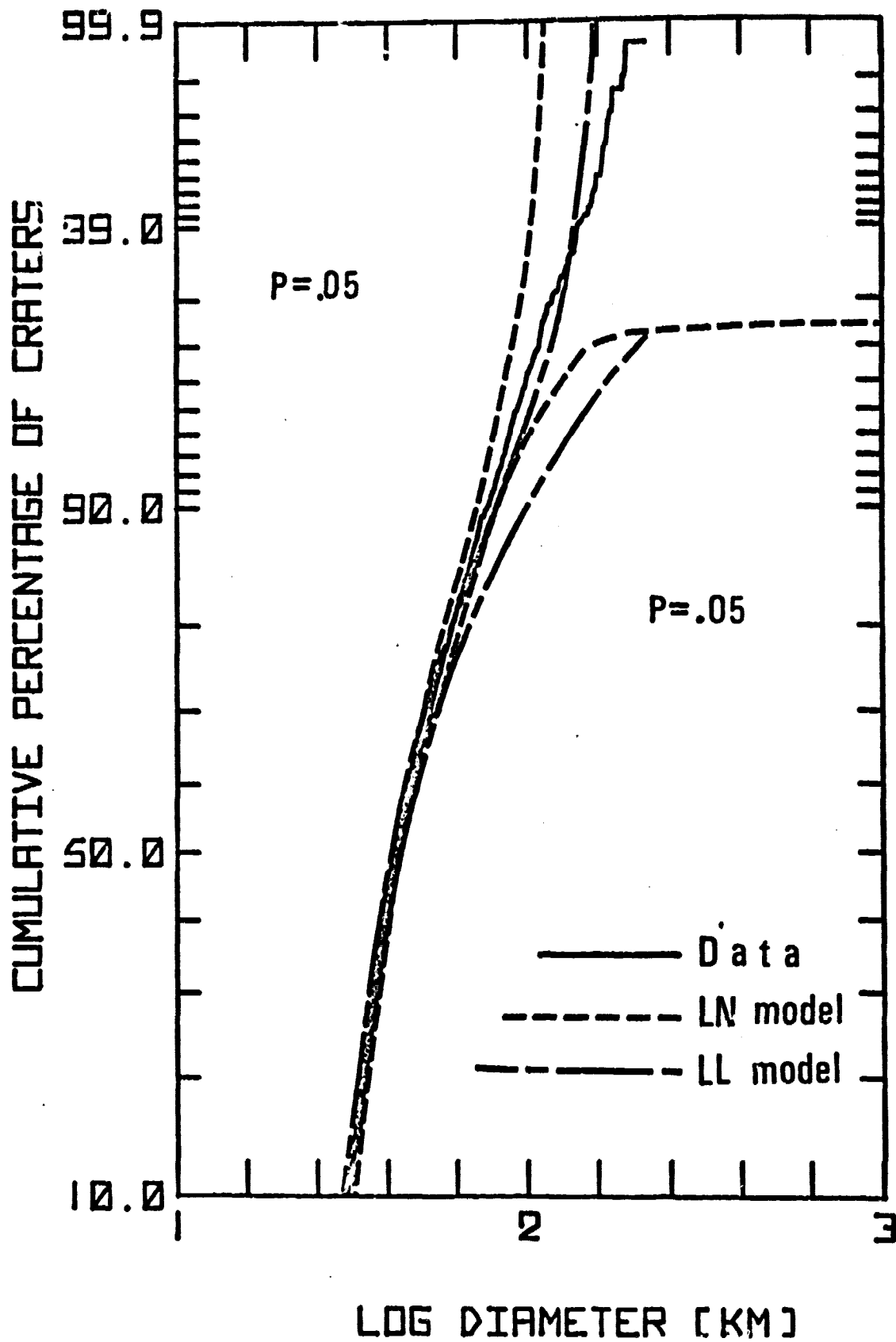


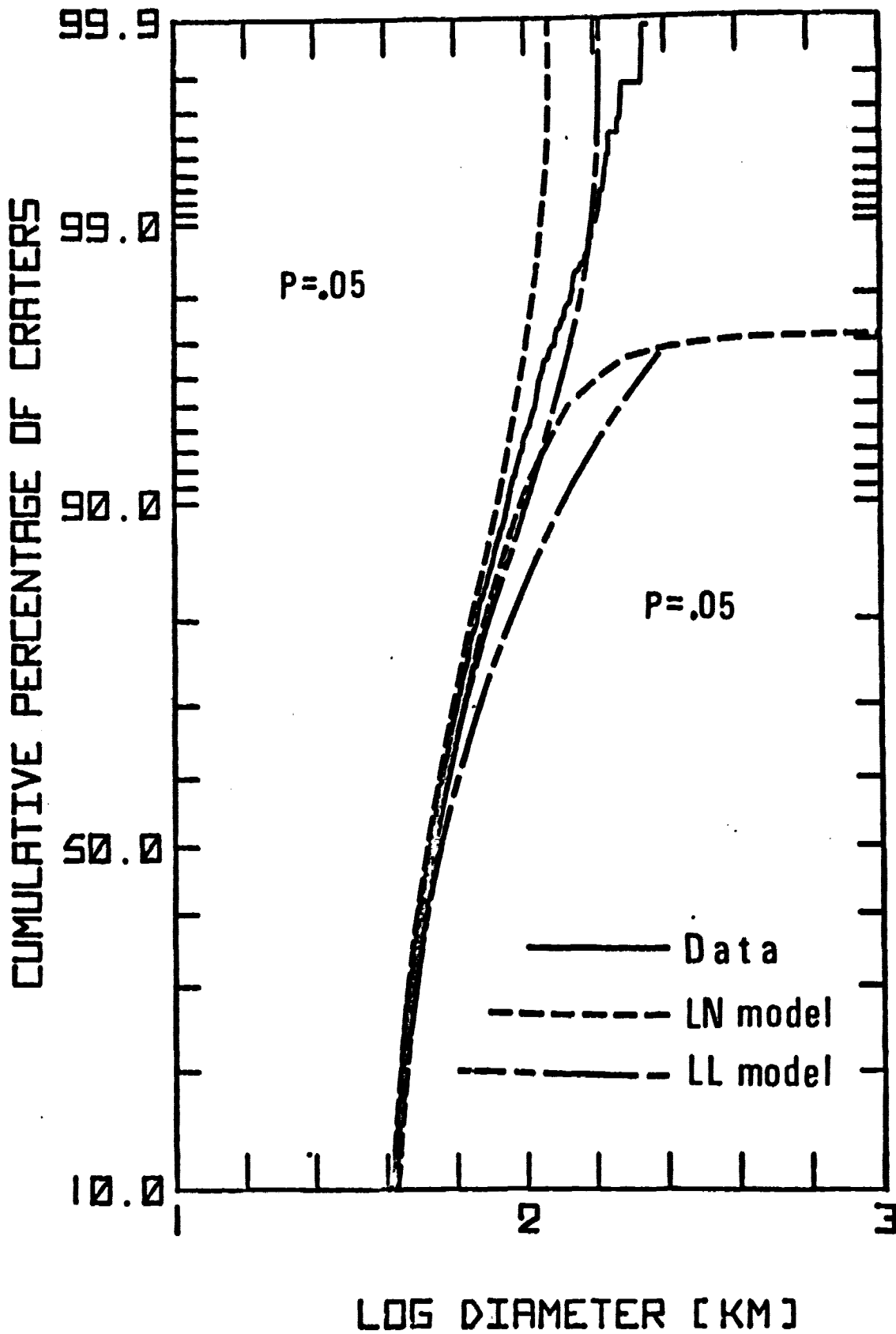
LOG CRATER FREQUENCY PER SQ KM



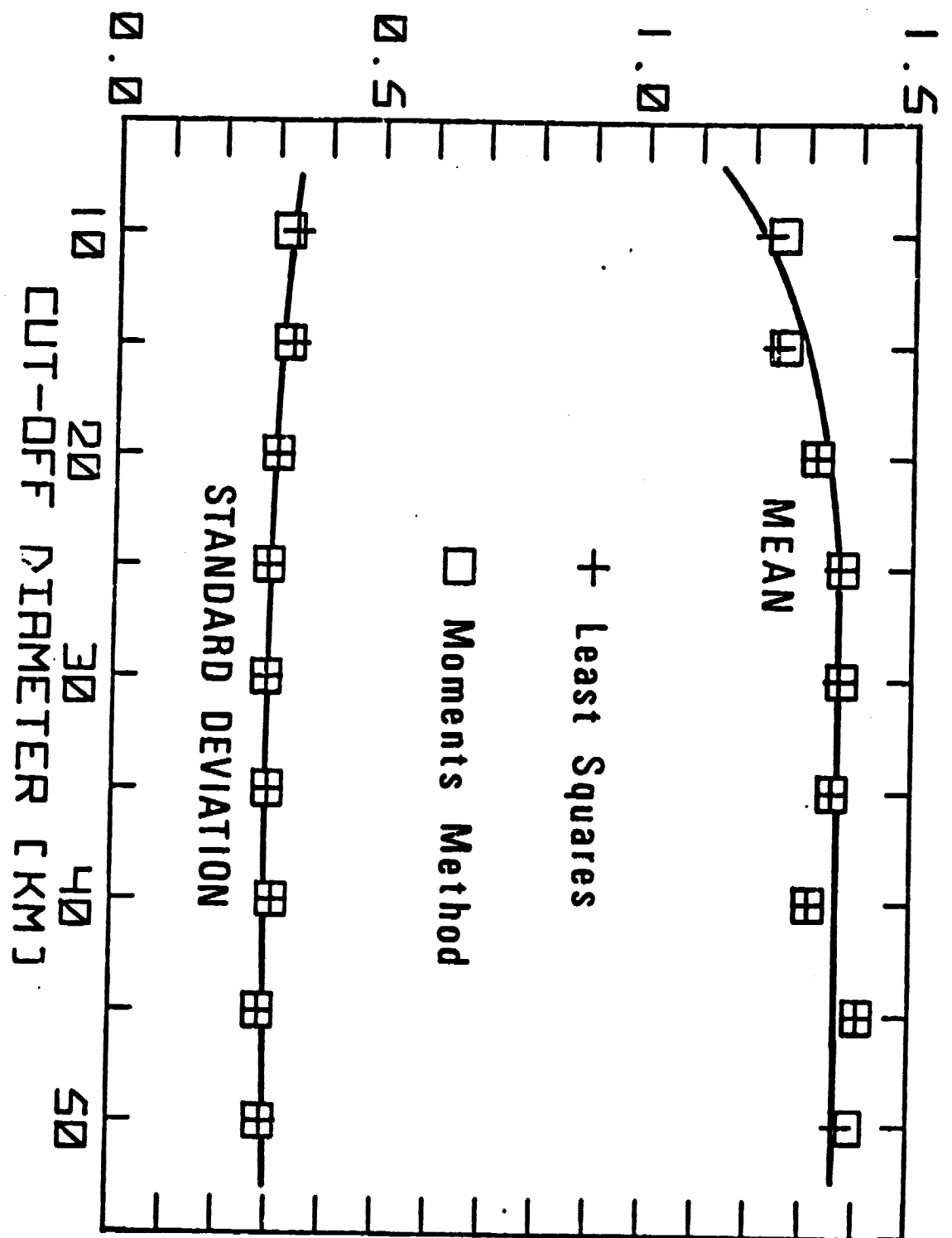


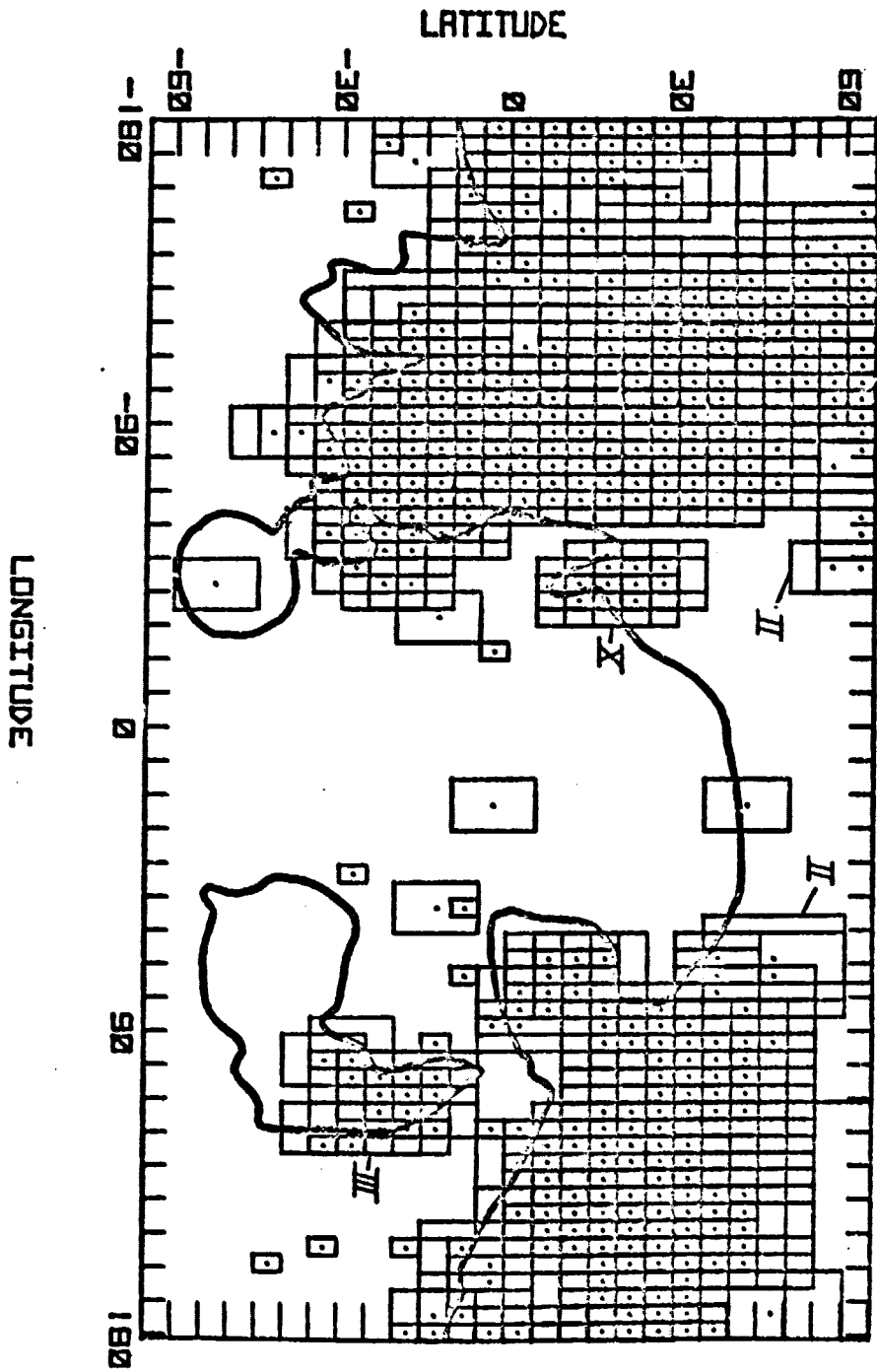


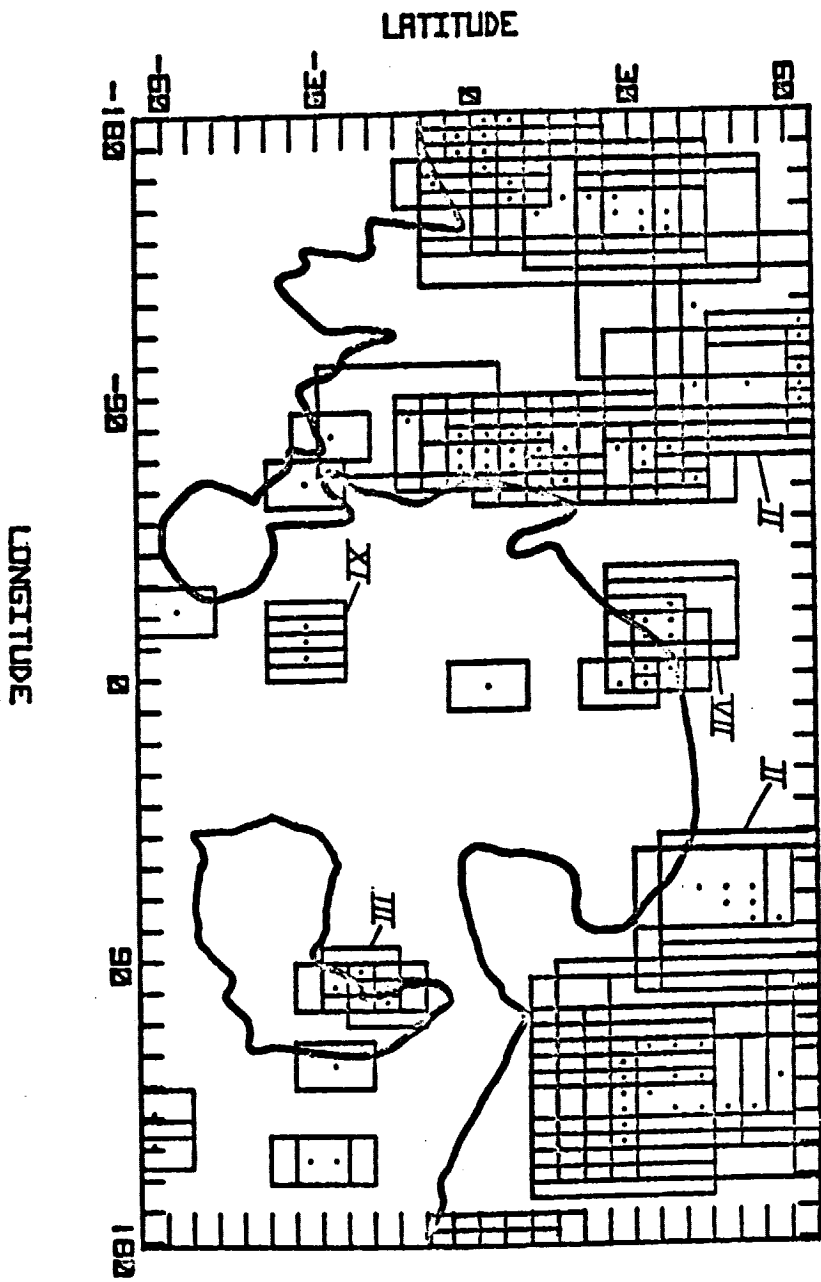




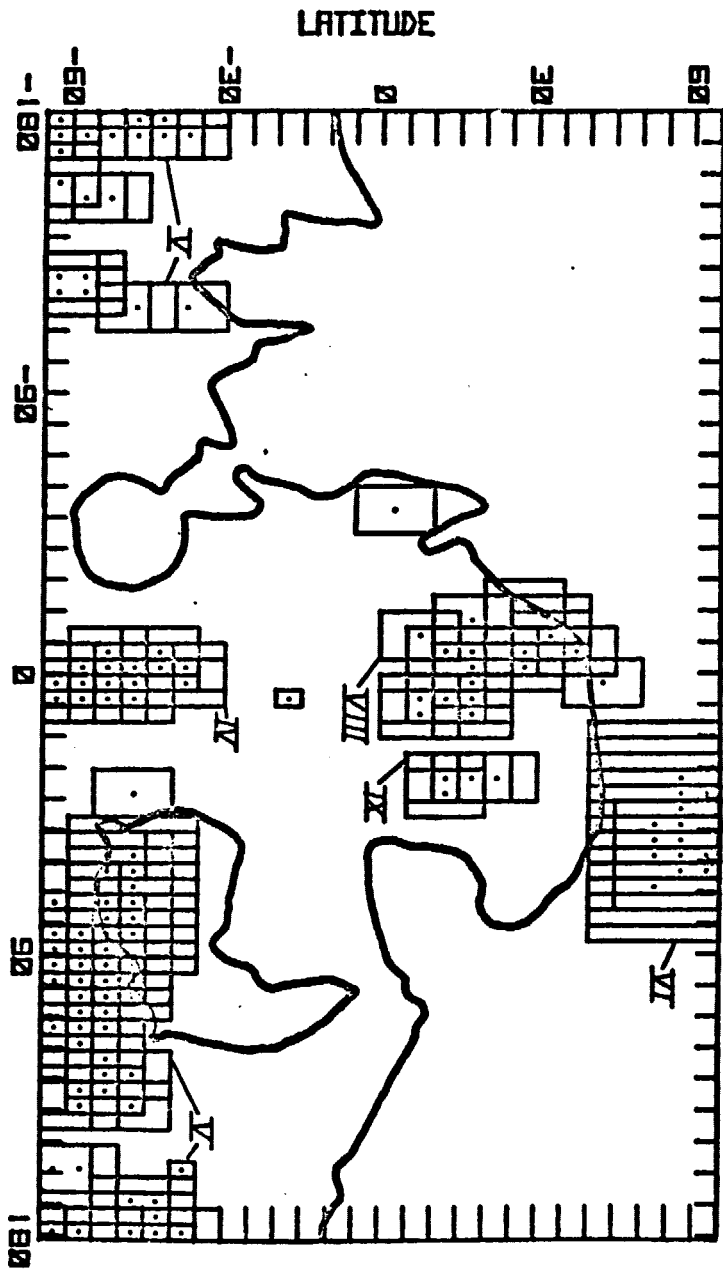
DISTRIBUTION PARAMETER VALUES





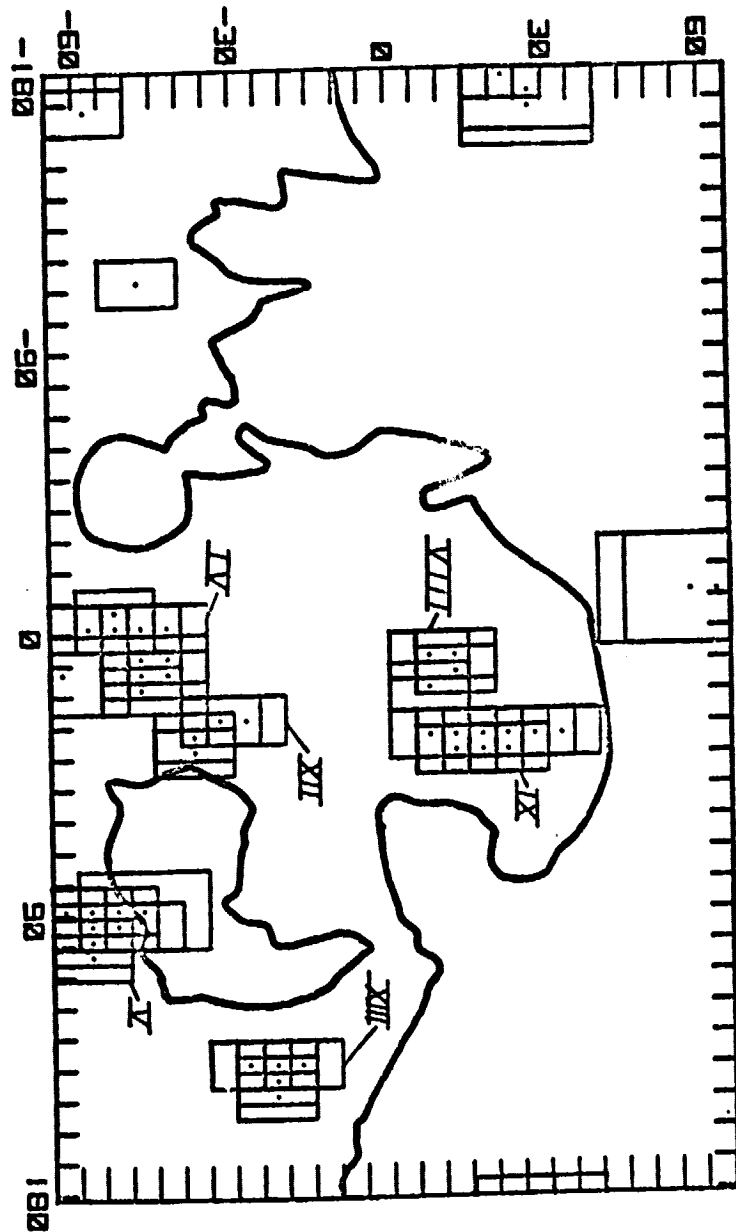


LONGITUDE



LONGITUDE

LATITUDE



LONGITUDE

